The International Journal of Advanced Manufacturing Technology (2021) 115:3579–3587
https://doi.org/10.1007/s00170-021-07367-x

ORIGINAL ARTICLE

Study on the formation and prevention mechanism of internal voids in cross wedge rolling

Zhi Jia[1,2] · Baolin Wei[1] · Xuan Sun[1]

Received: 13 January 2021 / Accepted: 28 May 2021 / Published online: 8 June 2021

Abstract

A three-dimensional numerical simulation model of cross wedge rolling (CWR) was developed to analyze the influence law of die parameters on internal voids during CWR using a rigid-plastic finite element method (FEM), where particular attention has been given to the internal void generation mechanism during CWR of shaft parts from the analyses of morphology, stress, and strain. The main reason for the internal voids during CWR is the extremely uneven deformation of the core and surface of the rolled product. By adjusting the key die parameters in CWR, the influence of die process parameters on internal voids in CWR was studied. As a result, the larger the forming and widening angles, the smaller the diameter of the rolled workpiece after rolling, and when the distribution coefficient of area reduction is about 1, the more difficult it is for loose defects to occur. According to the simulation results, a new CWR die structure was proposed and rolling experiments were performed. No looseness was found in the center, which proved that optimizing the die was feasible.

Keywords Cross wedge rolling (CWR) · Internal voids · Numerical simulation · Die paraments · Connecting rod

1 Introduction

Cross wedge rolling (CWR) is an efficient method for forming parts, which is widely used in the forming of step shaft and rod parts, and also used as a blank-making process in the forging process. [1–4] Compared with other machining methods, cross wedge rolling has characteristics of high forming accuracy, high production efficiency, good production environment, and low equipment investment. [5] There are many kinds of CWR methods, of which the most widely used is twice-stage cross wedge rolling. Although CWR has many advantages, its die design is difficult, the deformation law of the material during rolling is complicated, and the contact state between the die and the material is difficult to predict, which limits wide applicability of CWR. [6] The biggest limitation is that void defects are easily generated in the center of the billet during the CWR process, which affects the product performance.

Since the invention of the CWR process, internal voids have been the research focus. Scholars have conducted a lot of research on this problem through physical simulation, theoretical analysis, numerical simulation, and other methods, but its mechanism is not clear yet. There is no complete agreement on the primary mechanism of internal voids. Li et al. [7, 8] summarized the primary explanations as follows: (1) excessive shear stresses induced by the knifing action of the forming dies; (2) large tensile stresses in the central portion of the workpiece; and (3) the development of low cycle fatigue during the rolling process. The analysis of metal forming in the two-roll cross wedge rolling process using finite element method was assessed by Wang et al. [9] Silva et al. analyzed the damage evolution during cross wedge rolling of steel DIN 38MnSiVS5. [10] Pater [11, 12] studied the reasons for the defects in cross-rolled bars and concluded that the cavity formations were caused by shear and tensile stresses inside the workpiece. Zhou et al. [13] investigated a study on central crack formation in cross wedge rolling. The micromechanism of central damage formation during cross wedge rolling was analyzed by Yang et al. [14] Liu et al. [15] researched the influence of reduction distribution on internal defects during the cross wedge rolling process.

✉ Zhi Jia
jiazhi@lut.edu.cn

[1] School of Material Science and Engineering, Lanzhou University of Technology, Lanzhou, Gansu Province, China

[2] State Key Laboratory of Advanced Processing and Recycling of Nonferrous Metals, Lanzhou University of Technology, No. 287 Langongping Road, Qilihe District, Lanzhou, Gansu Province 730050, People's Republic of China

From the above analysis, it can be seen that scholars' research focuses on the flow law of materials, defect generation mechanism, and defect prediction, where each applies to the plastic mechanics method to analyze and predict the voids. However, these methods use mechanical parameters to indirectly analyze the generation mechanism and critical void conditions. In this paper, a three-dimensional numerical simulation model of CWR is established based on the rigid-plastic finite element method to study the generation mechanism of internal voids during CWR of shaft parts and analyze the influence law of mold parameters on the voids.

2 Finite element model

When a manufacturer uses the forging process to produce connecting rods, it first uses wedge rolling to make billets. Figure 1a shows the model of a roll workpiece. The overall structure belongs to the shaft parts, which is shown as half of the model due to the symmetry. Since the area reduction of each part of the rolled workpiece reaches 76.4%, it is necessary to carry out two rolling per part. After the rolling experiment, the rolled workpiece was cut longitudinally, which is found that the voids in part 4. The billet after rolling is shown in Fig. 1b. CWR is the process of complex, three-dimensional, large plastic deformation. The billet is at a high temperature and flows violently during the rolling process, from which compression, tensile, bending, shear, torsion, and other deformations occur at the same time. Moreover, the deformation is a periodic and non-uniform alternating process and the deformation time is very short, so it is difficult to observe the porosity defect generation process in the actual rolling process.

To accurately analyze the causes of porosity, a three-dimensional finite element method is used to study the deformation process of CWR. The CWR has many influencing factors, which is a process of material, geometrical, and boundary condition nonlinearity. It is difficult to directly analyze the process of internal voids only through the stress-strain relationship. To solve this problem, the good mesh characteristics of the Simufact-forming software were utilized; a three-dimensional numerical simulation model according to the actual process state was established. Using the symmetry of the workpiece, a numerical simulation analysis is performed on half of the structure of the workpiece. In this numerical model, the workpiece material is set as a plastic body, and the material such as a roll is set as a rigid body. After many numerical simulations and experimental verifications, a hole with a diameter of 5 mm is preset in the center of the blank. If the diameter of the center hole is less than 5 mm, there will be too many meshes in the numerical simulation process, which will cause the numerical simulation time to be too long; too large diameter of the center hole will affect the simulation accuracy, so the center hole diameter is set to 5 mm.Then, the change of the size of the hole was observed during the rolling process, which is the quantitative analysis of the process of the generation of voids. If the hole size after rolling is larger than 5 mm, it indicates that the central part will have void defects. The main process parameters of the manufacturer's original design plan are shown in Table 1.

Figure 2 shows the comparison between the results of the actual production and the numerical simulation. It can be seen that the billet shape after the actual production and numerical simulation is generally the same. To further verify the accuracy of the numerical simulation model, the diameters of the

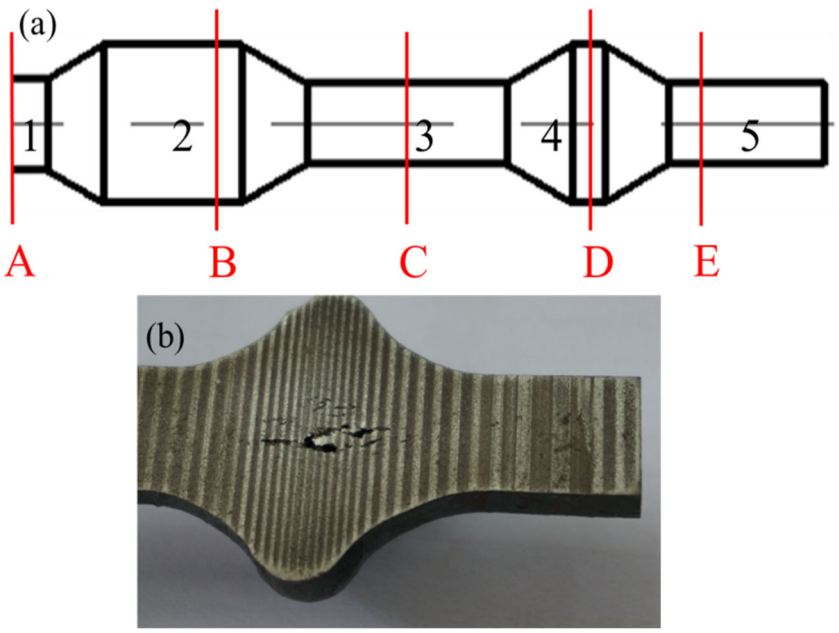

Fig. 1 **a** Model of a rolled workpiece. **b** The cross section of actual rolled workpiece

Table 1 Main parameters in the original design project

Parameter	Value
Rotational speed of roll/(r·min^{-1})	10
Initial temperature of tools/°C	20
Roll diameter/mm	630
Forming angle/(deg)	28
Spreading angle/(deg)	8
Total area reduction/(%)	76.41
Initial temperature of workpiece/°C	1100
Convection coefficient (N/s/mm/°C)	0.02
Heat transfer coefficient (N/s/mm/°C)	11
Material of workpiece	40Cr
Material of die	H13
Friction coefficient	1

typical cross sections of the actual parts and numerically simulated parts were measured, respectively. The locations of the cross sections are shown in Fig. 1a. As shown in Table 2, it can be seen that the average error between the simulation results and the actual production results is 1.82% and the maximum error is 4.6%. From the perspective of the cross section, the largest errors appear in sections E-E, and the remaining parts have errors less than 2%, indicating that the numerical simulation model established is consistent with the actual situation.

3 Results and discussion

3.1 Morphological analysis

As can be seen from Fig. 1b, the void defect at the center of the part 4 shows a significant distribution difference in the axial direction. On the side close to site 5, the central voids were more serious, while on the side close to site 3, the central voids were less. There are also differences in distribution on the

Table 2 Comparison of the experimental and FEM-simulated forging profiles

Section	Finite element size/mm	Experimental size/mm	Error/ %
A-A	18.85	19.2	1.8
B-B	36.18	36.9	2
C-C	17.98	18.05	0.4
D-D	39.87	39.99	0.3
E-E	16.36	17.14	4.6

cross section, where large holes appear in the center, and with further distance from the center, the holes become smaller.

Figure 3 shows the evolution of the voids in the numerical model of a rolled workpiece during the rolling process when the original design of the enterprise is simulated. From Fig. 3, the hole diameter of part 4 starts to increase when rolling part 5 in the first pass, and when rolling part 5 in the second pass, the hole expansion is more obvious. It is observed that when rolling part 3 in the second pass rolling, the diameter of the hole rapidly increases until the rolling is completed. It can be seen that in different rolling stages, the change trend of the hole evolution is different, and the change is related to the degree of accumulation of the material at different parts. The greater the resistance, the more severe the cavity expansion.

To further understand the change process, the change of the hole diameter during rolling was calculated. Figure 3 also shows the change in the diameter of the holes during rolling part 4 of the workpiece. In the figure, the first stage is part 1 of the rolled workpiece, the second stage is part 1 in the first rolled pass, the third stage is part 5 in the first rolled pass, and the fourth stage is part 5 in the second rolled pass. The fifth stage is part 3 in the second rolled pass. On the whole, as the rolling process progresses, the internal voids of the rolled billet gradually increase. Specifically, it can be seen from the figure that when the first rolling of part 5 is started, the diameters of the holes rapidly increase compared to that of the third stage, and then stop expanding until the rolling of the fifth stage is completed. Therefore, the first rolling of part 3 has a

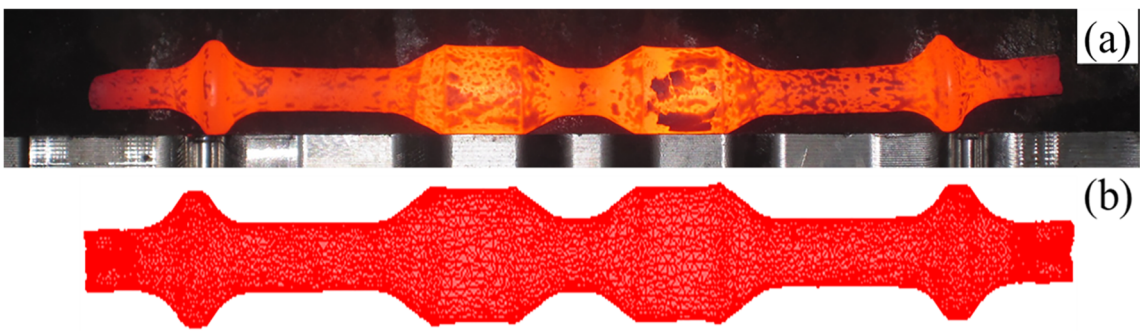

Fig. 2 Connecting rod workpiece after rolling. **a** Actual production of workpiece. **b** Numerical simulation of workpiece

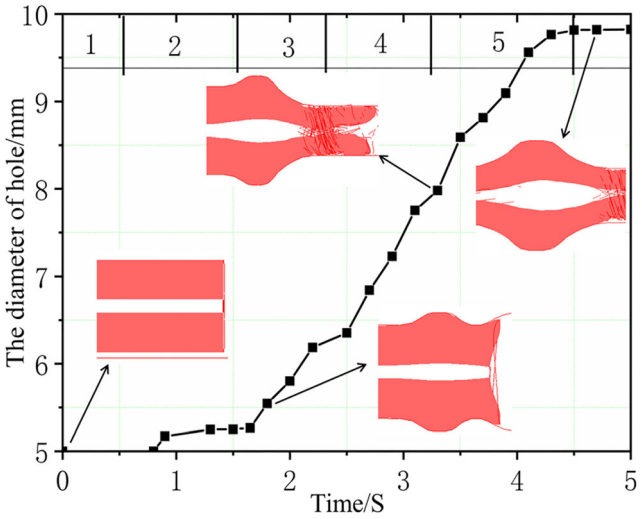

Fig. 3 The change of hole diameter and void evolution in the numerical model of the rolled workpiece

small effect on the expansion of the small head hole, while the two rolling times of part 5 and the second rolling of part 3 are the stages that have the greatest effect on the holes during the rolling process. The formation of part 5 obstructs the material to continue to flow in the axial direction, which causes the material gathered in part 4, resulting in the internal voids. Also, the greater the resistance of part 5 to the axial flow of the material, the greater the risk of generating voids at part 4.

3.2 Stress analysis

To analyze the stress of different parts during the CWR process, four characteristic points were taken on the longitudinal section of part 4, as shown in Fig. 4. Figure 5 shows the change curve of the stress of part 4 during the CWR process. As can be seen from Fig. 5, the maximum principal stress fluctuates around the zero line, and the amplitude of the fluctuation is relatively large. At the beginning of the rolling process, the rolled workpiece is almost in a tensile stress state, and the tensile stress at center point P2 is always greater than other characteristic points. As the rolling process progresses, the surface of the rolled workpiece is in a state of gradual compressive stress, while the central part is always in a state of tensile stress, and the stress at P3 is greater than that at P1. The variation trend of shear stress is similar to that of principal stress. By observing the deformation process, it was found that the stress at characteristic point P2 reaches a maximum value when the first rolling is performed on part 5, which was consistent with the change law of the holes in Fig. 3. From the above analysis, it can be seen that the stress in part 4 is very uneven, and the stress area is mainly concentrated in the center, while the stress on the surface is very small. Concurrently, the center is in a state of negative hydrostatic stress for a long time, making the center the most vulnerable position and prone to void defect generation. During repeated rolling in the CWR process, the cyclic alternating shear stress causes micro-cracks to occur in the weak center of the rolled workpiece. Under the slip action, the micro-cracks grow and gather constantly in the rolling process. The alternating tensile stress promotes the development of micro-cracks, which leads to fracture separation and forms a macroscopic fracture.

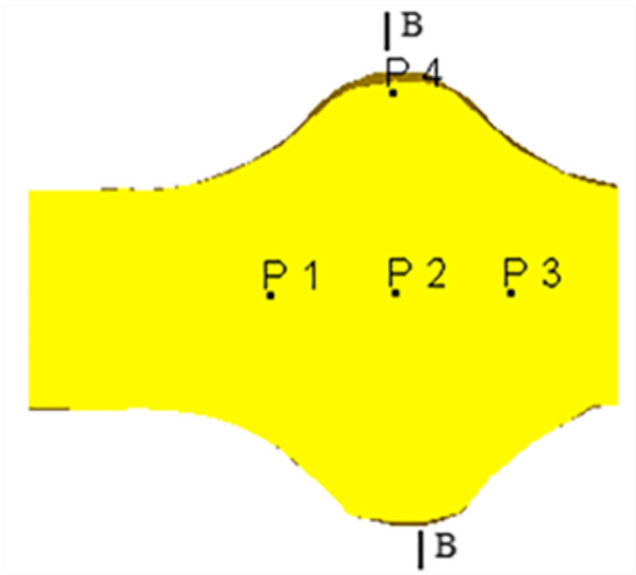

Fig. 4 Schematic diagram of the location of feature points

3.3 Strain analysis

Strain is a variable used to characterize the degree of material deformation. Figure 6 shows the variation law of strain at characteristic points with respect to time in the CWR process. It can be seen from Fig. 6 that the maximum principal strains at the points of the small head portion are all positive values, indicating that the deformation in the principal direction of the portion is a tensile deformation. The maximum principal strain fluctuation at the center point is relatively small, and reaches the maximum at 3.28 S. At this time, the second rolling is started on part 3 of the workpiece. Under the action of the oblique wedge, the material suddenly starts to flow outward so that the outside of the small head of part 4 is in contact with the mold, so part 4 is deformed, which indicates that the degree of deformation of part 3 has a great influence on the deformation of the part 4. The maximum principal strain at surface point P4 gradually increased during the fluctuation, and starting from the second pass of rolling on part 5 of the workpiece at 2.35S, the amplitude of fluctation of the maximum principal strain gradually increased and reached a maximum at 3.54 S. The maximum principal strain at center point P2 is the smallest. However, at point P1, where the material enters the small head, and point P3, which flows out of the small head, the maximum principal strains are both greater

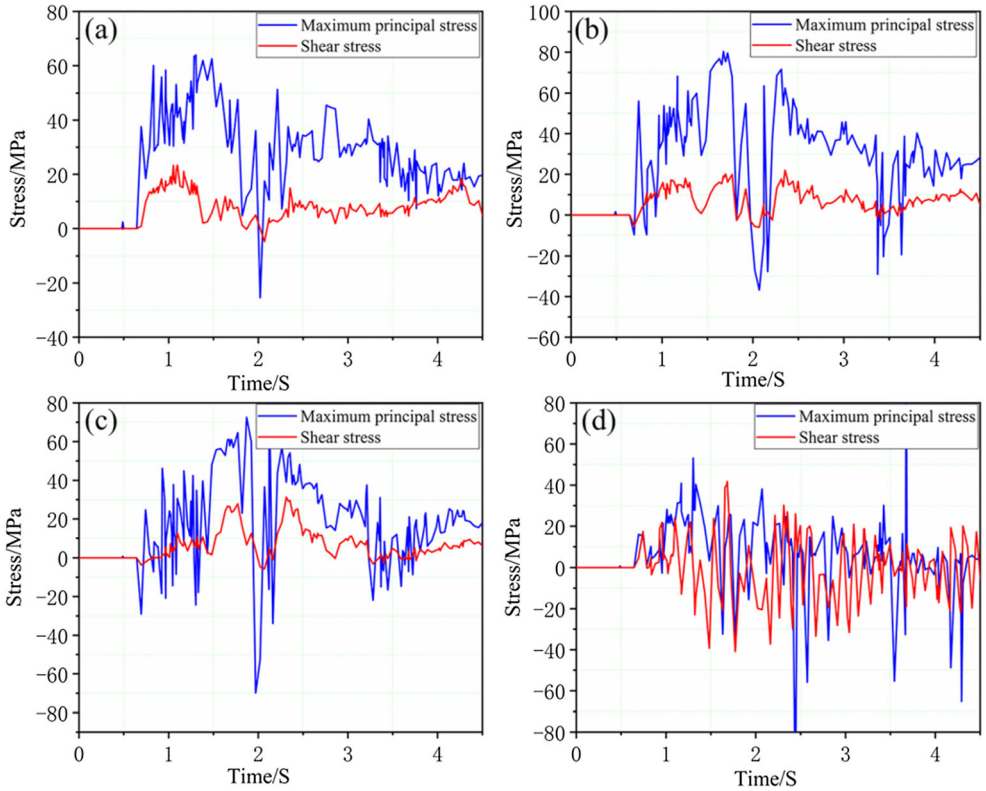

Fig. 5 Stress analysis at feature points. **a** P1. **b** P2. **c** P3. **d** P4

than at point P2, and the deformation at point P3 is the largest, which is consistent with the distribution pattern of the voids. The maximum principal strain at P4 is much larger than the center, which indicates that the surface deformation is much

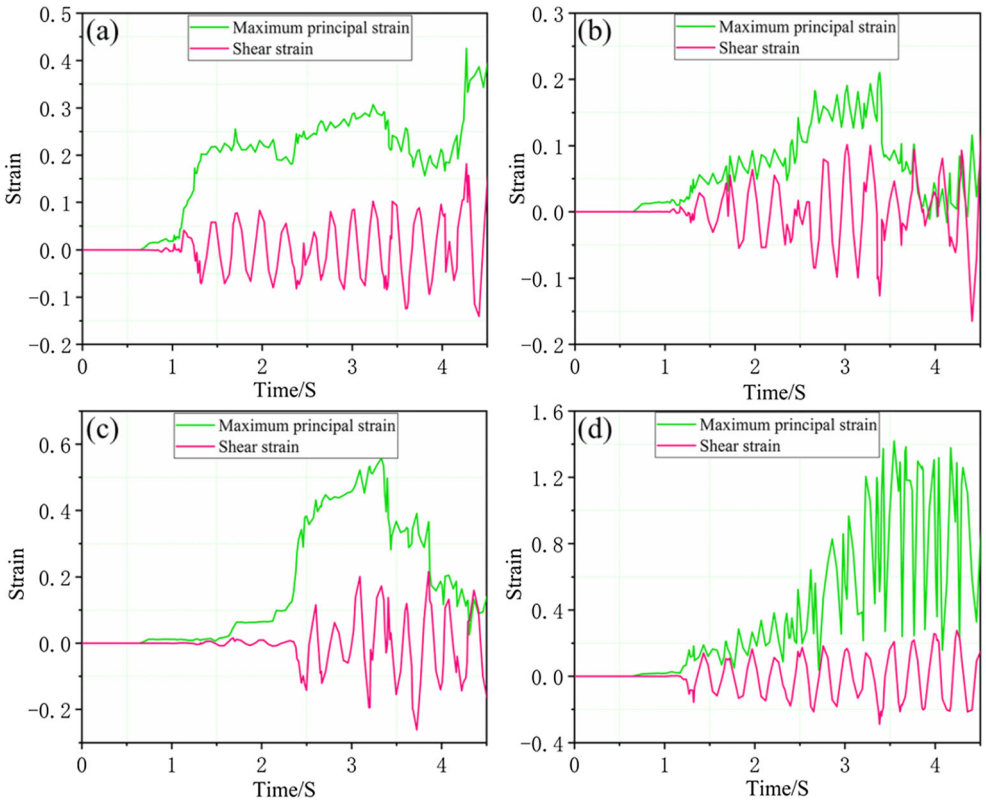

Fig. 6 Strain analysis at feature points. **a**P1. **b** P2. **c** P3. **d** P4

Table 3 Simulation parameters

Experiment	Forming angle (°)	Widening angle (°)	The distribution coefficient of area reduction	Diameter of part 4 (mm)
1	20, 23, 26, 29, 32	8	0.96	31
2	29	4, 6, 8, 10, 12	0.96	31
3	29	8	0.53, 0.73, 0.96, 1.3, 1.56	31
4	29	8	0.96	25, 28, 31, 33, 36

more severe than the center, and the shear strain also shows similar characteristics. From the above analysis, it can be seen that this part is in an extremely deformed and uneven state during the CWR process. The oblique wedge corresponding to part 5 hinders the material flow of part 4, which promotes the sharp deformation of the surface material of part 4, but the center shows that no deformation has occurred. The extremely uneven deformation caused a large alternating tensile stress in the center. When the tensile stress reached the yield limit, micro-cracks developed and gradually became the macroscopic internal voids.

3.4 Effect of die parameters

From the perspective of mechanics, the internal voids during the CWR process are caused by the local stress and strain of the material, and the geometry and process parameters of the CWR die are decisive in relation to mechanical parameter change. The forming angle α, widening angle β, and area reduction ΔA are the key die parameters in CWR. These parameters not only determine the severity of plastic deformation but are also the decisive factors in the occurrence of internal voids.

To avoid the occurrence of internal void defects in the CWR process, the relationship between die parameters and material deformation characteristics must be studied. According to theoretical research and experimental results, the range of forming angle α is 18–34°, the range of widening angle β is 4–12°, and the range of area reduction ΔA is 35–75% during the CWR process. To analyze the relationship between the size effect of the rolled workpiece and the internal voids, the diameter of the rolled workpiece of part 4 was also

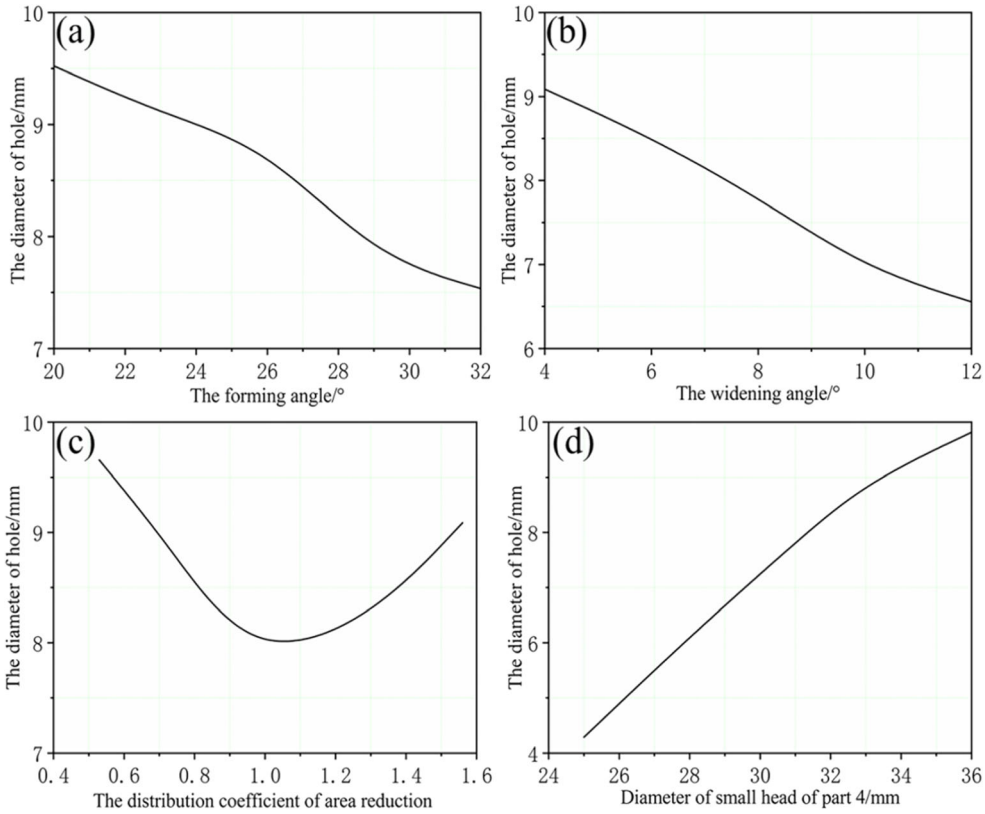

Fig. 7 Influence of mold parameters on the diameter of hole

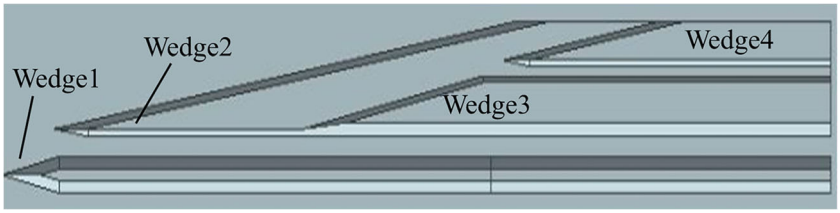

Fig. 8 Optimized CWR die

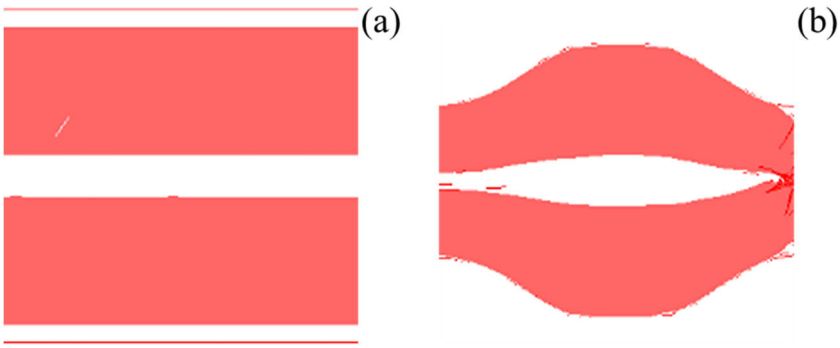

Fig. 9 Simulation results of hole changes after CWR. **a** Before deformation. **b** After deformation

analyzed as a variable in this study. In this paper, the diameter change of the 5-mm diameter hole that is set in advance at the center of billet was analyzed to study the influence of process parameters on the void defects during CWR. The simulation experiments between die parameters and material deformation are divided into four groups, and the experimental parameters are shown in Table 3.

Figure 7 shows the influence of CWR die parameters on the hole diameter. It can be seen from the figure that the forming angle α and widening angle β increase, and the diameter of the hole becomes smaller, which indicates that when these two parameters are selected to a larger value, it is beneficial for the uniform deformation of the surface layer and the center of the billet, and it is favorable to suppress the internal voids. In Fig. 7a, when the forming angle α is in the range of $26 \sim 30°$, the change in the diameter of the hole is large, while outside this range, the change is relatively little. So, this range should be avoided when selecting parameters. It can be seen from Fig. 7b that the influence of the widening angle β on the diameter of hole is basically linear, which indicates that the diameter of the hole is relatively sensitive to the change of the widening angle β, and the influence of the widening angle on the internal voids is greater than that of the forming angle. Figure 7c shows the effect of the distribution coefficient of area reduction on the cavity diameter, which indicates that the curve is parabolic. When the distribution coefficient of area reduction is around 1, the diameter of the hole minimized. When the distribution coefficient of area reduction is less than 1, the change in the diameter of the hole is relatively large, indicating that the deformation of the second rolling has a great effect on the internal voids, and the larger the second rolling deformation, the more serious the internal voids. In Fig. 7d, it can be seen that the larger the diameter of part 4 after rolling, the larger the diameter of hole, and the diameter of hole increases linearly. As a whole, the effect of the diameter of part 4 on the diameter of the hole is the largest. When the diameter of part 4 is small enough after rolling, the diameter of the hole is even less than 5 mm, indicating that the compression deformation is strong in this case, and even micro-cracks will be pressed together.

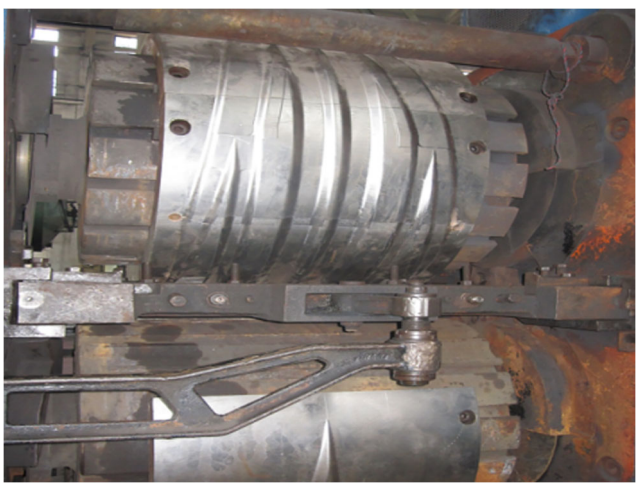

Fig. 10 Cross wedge rolling die and equipment

4 Optimization and industrial application of cross wedge rolling die

From the above analysis of the industrial problem, it was found that the internal void defects generated at part 4 of the

Fig. 11 Rolled pieces after cutting

rolled workpiece originated from the severe uneven deformation of the part during the CWR process, which caused the material to restrict outward flow. To completely solve this problem, a new CWR die structure is proposed, and its structure is shown in Fig. 8. The characteristics of this die structure show that the rolling sequence expands from the inside to the outside, and the outward flow of the billet is always unhindered, which greatly reduces void defect occurrences and simplifies the stress of the billet during the rolling. According to the results obtained in Section 3.4, the distribution coefficient of area reduction of the die structure is 0.97, the forming angle is 30°, the widening angle is 8°, and the diameter of part 4 of the rolled workpiece is 25 mm.

The new die structure was analyzed using the numerical simulation model established in this paper. The simulation results are shown in Fig. 9. Analysis and simulation results found that the diameter of the internal voids after rolling was 4.7522 mm, which was smaller than the preset hole diameter of 5 mm, indicating that the center of the small head did not expand, and the position met the design requirements. To verify the results, rolling experiments were performed using a D46-1000 wedge rolling mill, as shown in Fig. 10. The rolled sample was cut on the longitudinal section, and no internal voids were found in the center, indicating that the optimization scheme is feasible, as shown in Fig. 11.

5 Conclusion

By tracking the size of the cavity inside the rolling piece, the influence of the mold parameters on the center gap of the rolling piece is studied. Based on numerical simulation and production verification, the following conclusions were drawn:

1. In the process of CWR, internal void defects are prone to occur. The main reason is the extremely uneven deformation of the core and the surface of the rolled workpiece. At the same time, the core of the rolled workpiece to be in a state of negative hydrostatic stress, which was dominated by tensile stress. The cyclic alternating shear stresses cause micro-cracks to occur in this part. What's more, under the action of slip, micro-cracks continue to produce, grow, and aggregate during rolling process. The alternating tensile stress promotes the development of micro-cracks, which leads to fracture separation and forms macroscopic fracture.
2. The internal voids are related to the size of the forming and widening angles. With the larger forming and widening angles, the diameter of the hole in the rolled workpiece was smaller. Also, when the distribution coefficient of area reduction was about 1, it was difficult for the loose defects to occur.

Author contribution All the authors participated in and agreed to publish this article, and provided a lot of help in the process of writing this article.

Funding This study received support from the National Nature Science Foundation of China (No. 51665032), Science Foundation for Distinguished Young Scholars of Gansu Province (Grant No. 18JR3RA134), and Lanzhou University of Technology Support Plan for Excellent Young Scholars (Grant No. CGZH001).

Availability of data and materials The data, materials, and related pictures in this article are true and available.

Declarations

Consent to participate With consent.

Consent to publish With consent.

Conflict of interest The authors declare no competing interests.

References

1. Huo YM, Lin JG, Bai Q, Wang BY, Tang XF, Ji HC (2017) Prediction of microstructure and ductile damage of a high-speed railway axle steel during cross wedge rolling. J Mater Process Technol 239:359–369. https://doi.org/10.1016/j.jmatprotec.2016.09.001
2. Pater Z (2000) Theoretical and experimental analysis of cross wedge rolling process. Int J Mach Tool Manu 40(1):49–63. https://doi.org/10.1016/S0890-6955(99)00047-4
3. Qiang YF, Song PB (2007) Analysis on temperature distribution in cross wedge rolling process with finite element method. J Mater

Process Technol 187:392–396. https://doi.org/10.1016/j.jmatprotec.2006.11.193
4. Wang MT, Li XT, Du FS, Zheng YZ (2005) A coupled thermal–mechanical and microstructural simulation of the cross wedge rolling process and experimental verification. Mater Sci Eng A 391(1-2):305–312. https://doi.org/10.1016/j.msea.2004.08.080
5. Li Q, Lovell MR (2004) The establishment of a failure criterion in cross wedge rolling. Int J Adv Manuf Technol 24:180–189. https://doi.org/10.1007/s00170-003-1607-0
6. Fu XP, Dean TA (1993) Past developments, current applications and trends in the cross wedge rolling process. Int J Mach Tool Manu 33(3):367–400. https://doi.org/10.1016/0890-6955(93)90047-X
7. Li Q, Lovell MR, Slaughter W, Tagavi K (2002) Investigation of the morphology of internal defects in cross wedge rolling. J Mater Process Technol 125(s1):248–257. https://doi.org/10.1016/S0924-0136(02)00303-5
8. Li Q, Lovell MR (2008) Cross wedge rolling failure mechanisms and industrial application. Int J Adv Manuf Technol 37(3-4):265–278. https://doi.org/10.1007/s00170-007-0979-y
9. Wang MT, Li XD, Du FS (2009) Analysis of metal forming in two-roll cross wedge rolling process using finite element method, Journal of Iron and Steel Research. International 16(1):38–43. https://doi.org/10.1016/S1006-706X(09)60008-X
10. Silva MLN, Pires GH, Button ST (2011) Damage evolution during cross wedge rolling of steel DIN 38MnSiVS5. Proc Eng 10:752–757. https://doi.org/10.1016/j.proeng.2011.04.125
11. Bartnicki J, Pater Z (2004) The aspects of stability in cross-wedge rolling processes of hollowed shafts. J Mater Process Technol 155-156:1867–1873. https://doi.org/10.1016/j.jmatprotec.2004.04.278
12. Pater Z (2006) Finite element analysis of cross wedge rolling. J Mater Process Technol 173:201–208. https://doi.org/10.1016/j.jmatprotec.2005.11.027
13. Zhou XY, Shao ZT, Pruncu CI, Hua L, Balint D, Lin JG, Jiang J (2020) A study on central crack formation in cross wedge rolling. J Mater Process Technol 279. https://doi.org/10.1016/j.jmatprotec.2019.116549
14. Yang CP, Dong HB, Hu ZH (2018) Micro-mechanism of central damage formation during cross wedge rolling. J Mater Process Technol 252:322–332. https://doi.org/10.1016/j.jmatprotec.2017.09.041
15. Liu GH, Zhong ZP, Shen Z (2014) Influence of reduction distribution on internal defects during cross-wedge-rolling process. Proc Eng 81:263–267. https://doi.org/10.1016/j.proeng.2014.09.161